ACS chemical biology

Articles

pubs.acs.org/acschemicalbiology

Comparative Chemogenomics To Examine the Mechanism of Action of DNA-Targeted Platinum-Acridine Anticancer Agents

Kahlin Cheung-Ong,[†] Kyung Tae Song,[‡] Zhidong Ma,[§] Daniel Shabtai,[∥] Anna Y. Lee,[†] David Gallo,[⊥] Lawrence E. Heisler,[‡] Grant W. Brown,[⊥] Ulrich Bierbach,*[,§] Guri Giaever,[‡] and Corey Nislow*[,†]

[†]Department of Molecular Genetics and the Donnelly Centre, [‡]Department of Pharmaceutical Sciences and the Donnelly Centre, [∥]Department of Cell and Systems Biology and the Donnelly Centre, and [⊥]Department of Biochemistry and the Donnelly Centre, University of Toronto, Toronto, ON, M5S3E1 Canada

[§]Department of Chemistry, Wake Forest University, Winston-Salem, North Carolina 27109, United States

Supporting Information

ABSTRACT: Platinum-based drugs have been used to successfully treat diverse cancers for several decades. Cisplatin, the original compound of this class, cross-links DNA, resulting in cell cycle arrest and cell death *via* apoptosis. Cisplatin is effective against several tumor types, yet it exhibits toxic side effects and tumors often develop resistance. To mitigate these liabilities while maintaining potency, we generated a library of non-classical platinum-acridine hybrid agents and assessed their mechanisms of action using a validated genome-wide screening approach in *Saccharomyces cerevisiae* and in the distantly related yeast *Schizosaccharomyces pombe*. Chemogenomic profiles from both *S. cerevisiae* and *S. pombe* demonstrate that several of the platinum-acridines damage DNA differently than cisplatin based on their requirement for distinct modules of DNA repair.

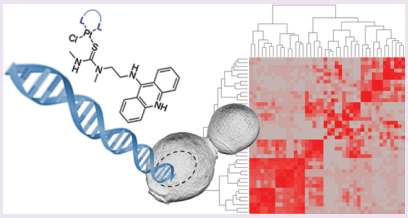

Platinum-based drugs are extremely successful cancer chemotherapeutics. The widely used agent cisplatin (*cis*-diamminedichloroplatinum(II)) acts by forming cross-links in the major groove of DNA that inhibit DNA synthesis and lead to apoptosis.[1] Cisplatin is effective against testicular, ovarian, bladder, and cervical tumors, but it manifests dose-limiting toxicities on the nervous and renal systems. Equally troubling is the frequency at which resistance develops during treatment.[2] In light of these limitations, attention has focused on developing platinum-based agents with improved activity in notoriously cisplatin-resistant cancers.

Diverse designs for new platinum-based anticancer drugs have focused on modifying substituents surrounding the cisplatin core. Clinical data show that these compounds offer certain advantages over cisplatin, yet because their mechanism of action is similar to that of cisplatin at the nuclear level, they represent an incremental improvement.[3] Alternative approaches to platinum-based drug design, in contrast, do not adhere to all of the structural dictates of cisplatin.[4] For example, a non-classical trinuclear platinum agent, BBR3464 (Novuspharma/Cell Therapeutics), damages DNA in a radically different manner than cisplatin and showed efficacy against colorectal, pancreatic, and ovarian cancer through phase II clinical trials.[5]

Recently, a class of promising platinum-acridine conjugates was developed by combining the DNA-damaging features of a platinum complex with the DNA-intercalating properties of acridine-based chromophores. The prototype of this class of hybrid agents, PT-ACRAMTU(EN) ([PtCl(en)(ACRAMTU)] dinitrate salt, ACRAMTU = 1-[2-(acridin-9-ylamino)ethyl]-1,3-dimethylthiourea, en = ethane-1,2-diamine), shows a dose response similar or superior to that of cisplatin in several solid tumor cell lines.[6−8] In the DNA adducts produced by PT-ACRAMTU(EN), the metal forms a single coordinative bond with the nucleobase nitrogen while the ACRAMTU moiety intercalates into the base-pair step adjacent to the site of platination.[9] This results in a novel mechanism of DNA damage distinct from the DNA cross-linking characteristic of cisplatin. On the basis of these promising initial results, additional platinum-acridine compounds were synthesized with a focus on modifications to the prototypical PT-ACRAMTU(EN) structure (Figure 1).[10−12] Structure−activity relationship studies revealed PT-ACRAMTU(EN) analogues with up to 500-fold higher potency in non-small cell lung cancer (NSCLC) cells when compared to cisplatin. The promise offered by the platinum-acridines is clear, yet the cellular mechanism(s) of these dual-mode agents remains largely uncharacterized.

Here we use a validated cell-based chemical genomic assay to examine a library of platinum-acridine hybrid agents to characterize their cellular mechanism(s) of action and evaluate their potential as anticancer agents. We have previously shown that the *Saccharomyces cerevisiae* gene deletion collection is a powerful means to dissect the detailed mechanisms of action of functionally diverse DNA-damaging agents[13] by screening these agents against the complete pool of ∼4,800 barcoded non-essential deletion strains. In this study we apply a similar approach in both *S. cerevisiae* and the distantly related fission yeast *Schizosaccharomyces pombe* to dissect the mechanism(s) of action of these novel platinum-acridine conjugates. The results

Received: April 10, 2012
Accepted: August 28, 2012
Published: August 28, 2012

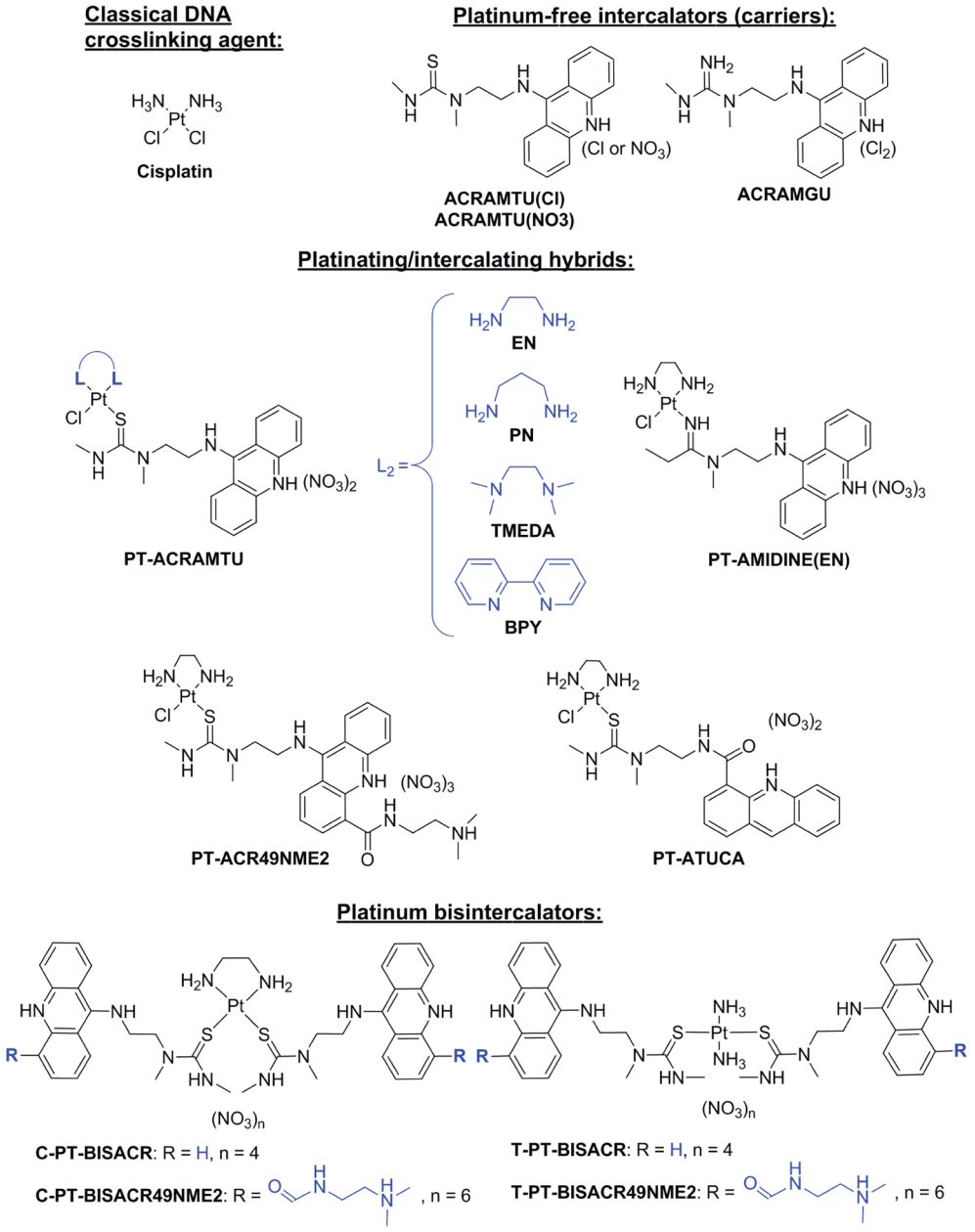

Figure 1. Chemical structures of the platinum-acridine compounds and carriers screened.

offer insight into the relative role of each structural modification on the genome-wide response and provide mechanistic insight into the relationship between compound structure and biological activity.

RESULTS AND DISCUSSION

Platinum-acridines derived from the prototype PT-ACRAMTU(EN) were developed using a modular synthetic approach. The compounds tested in this study can be grouped into three categories: platinum-free carriers (2 derivatives), platinating-intercalating hybrid agents (7 derivatives), and bisintercalators (4 derivatives) (Figure 1). Each genome-wide screen produces a fitness profile that consists of a numerical value for each deletion strain's fitness (relative growth with and without drug treatment) (Supplementary Data set 1). To compare genome-wide profiles between compounds, we used a rank-based similarity scoring algorithm developed to account for non-biological "batch"-based systematic effects.[14] With this algorithm, every gene deletion strain within a profile is distributed into sections, or "buckets", where strains that are most influenced by the chemical compound (and therefore have the highest fitness defect scores) comprise one bucket, the next set of strains are distributed into a second bucket, and so forth. Once all strains are divided into buckets, a scoring matrix is constructed and used to evaluate the similarity between profiles (see Methods). This approach effectively minimizes the influence of "batch" effects that can overwhelm the biological signal. Using the resulting profile similarity scores, compounds with similar mechanisms cluster together, with experimental replicates being the most similar (Figure 2).

Clustering of all *S. cerevisiae* profiles revealed that, of all the platinum-acridines, PT-ACRAMTU(EN) induces a cellular response most similar to that of cisplatin, further suggesting that the most significantly sensitive strains represent those

dx.doi.org/10.1021/cb300320d | *ACS Chem. Biol.* 2012, 7, 1892–1901

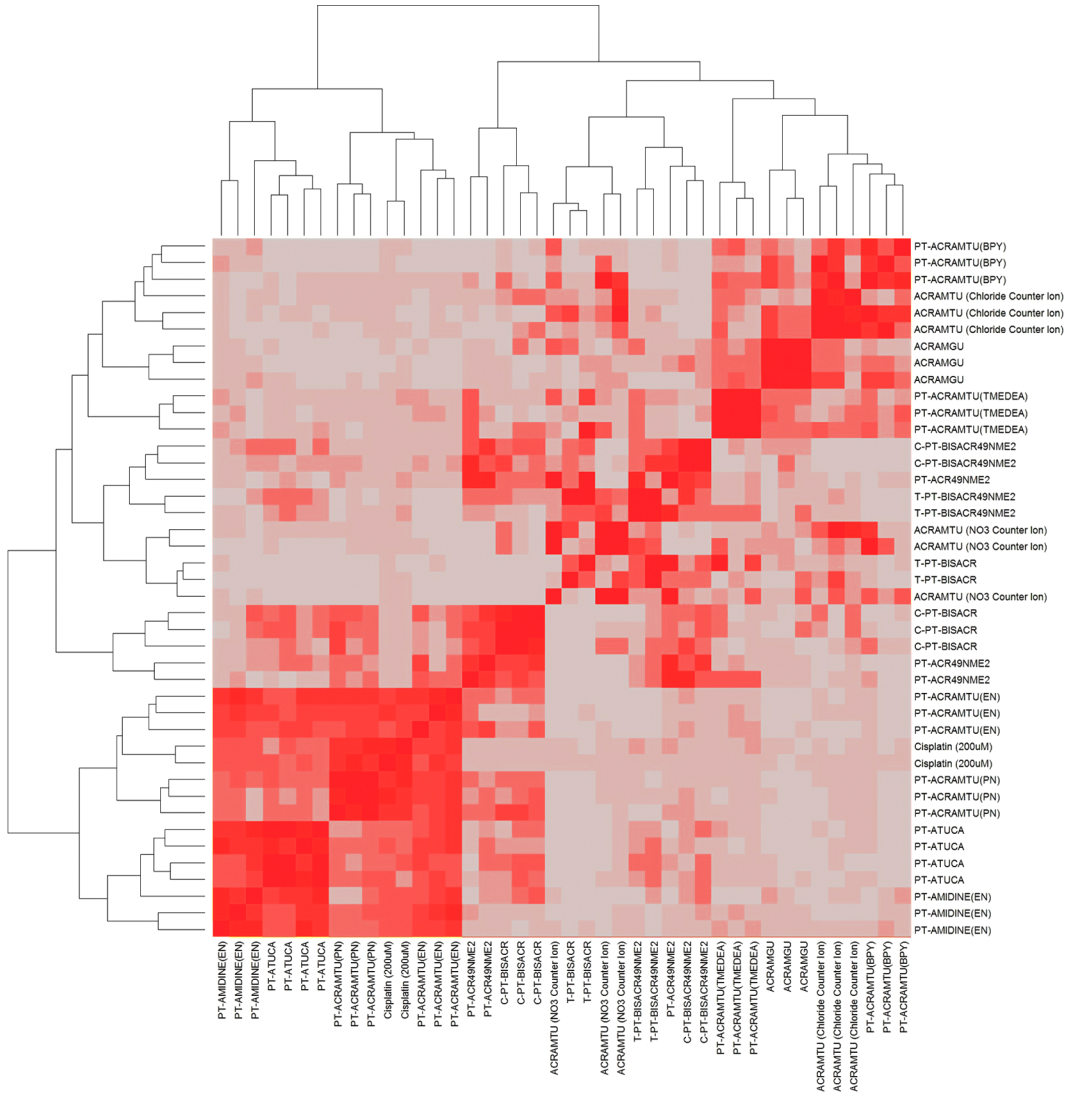

Figure 2. Two-dimensional hierarchical clustering of all 14 compounds based on the profile similarity scores of their genome-wide *S. cerevisiae* profiles. Red indicates high similarity between compound profiles, and gray indicates low similarity. Profiles from experiments repeated under the same conditions cluster together with few outliers, indicating the reproducibility and resolution of the genome-wide assay. The dendrogram reveals structure−function relationships between compounds.

deleted for genes involved in DNA-damage repair. PT-ACRAMTU(PN), PT-ATUCA, and PT-AMIDINE(EN) also grouped together with cisplatin and PT-ACRAMTU(EN). The platinum-free carriers and the 7 other platinum-acridine compounds clustered separately. Notably, PT-ACRAMTU-(BPY), which was previously examined for its DNA-damaging properties,[11] clusters with the platinum-free carriers, suggesting that it does not generate fitness defects in *S. cerevisiae*. The individual genome-wide strain sensitivities for each compound are discussed in detail below.

Cisplatin was profiled to serve as a benchmark for the platinum-acridines. We previously demonstrated that the cellular response to cisplatin requires genes with roles in nucleotide excision repair (NER), homologous recombination repair (HRR), post-replication repair (PRR), and translesion synthesis (TLS).[13] In this study, strains deleted for genes in NER (*RAD1*, *RAD2*, *RAD4*, *RAD10*, and *RAD14*), HRR (*RAD51*, *RAD52*, *RAD54*, *RAD55*, and *RAD57*), and PRR (*RAD5* and *RAD18*) were among the top 30 most cisplatin-sensitive strains. Strains deleted for *PSO2*, an NER gene involved in cross-link repair, and genes involved in TLS (*REV1*, *REV3*, and *REV7*) also ranked highly; these were previously found to be the principal differences in the response to well-characterized cross-linking and non-cross-linking agents.[13]

PT-ACRAMTU(EN) (Figure 1) forms monofunctional-intercalative adducts in both grooves of double-stranded DNA but does not cross-link nucleobases;[15] therefore we anticipated its genome-wide profile would be distinct from that of cisplatin. Contrary to this expectation, the DNA repair modules important for resistance to PT-ACRAMTU(EN) are most similar to those of cisplatin. The top 30 strains are deleted for genes in NER (*RAD1*, *RAD2*, *RAD4*, *RAD10*, and *RAD14*), HRR (*RAD51*, *RAD54*, and *XRS2*), and PRR (*RAD5* and *RAD18*) (Figure 3) with NER and PRR being the most sensitive modules (Figure 4a). One major difference from cisplatin is that deletion of *PSO2* did not sensitize this strain to PT-ACRAMTU(EN), suggesting that the monoadducts formed are not recognized by cross-link-specific repair mechanisms. In addition, genes essential for TLS were not found in the PT-ACRAMTU(EN) profile, as would be predicted for a non-

dx.doi.org/10.1021/cb300320d | *ACS Chem. Biol.* 2012, 7, 1892−1901

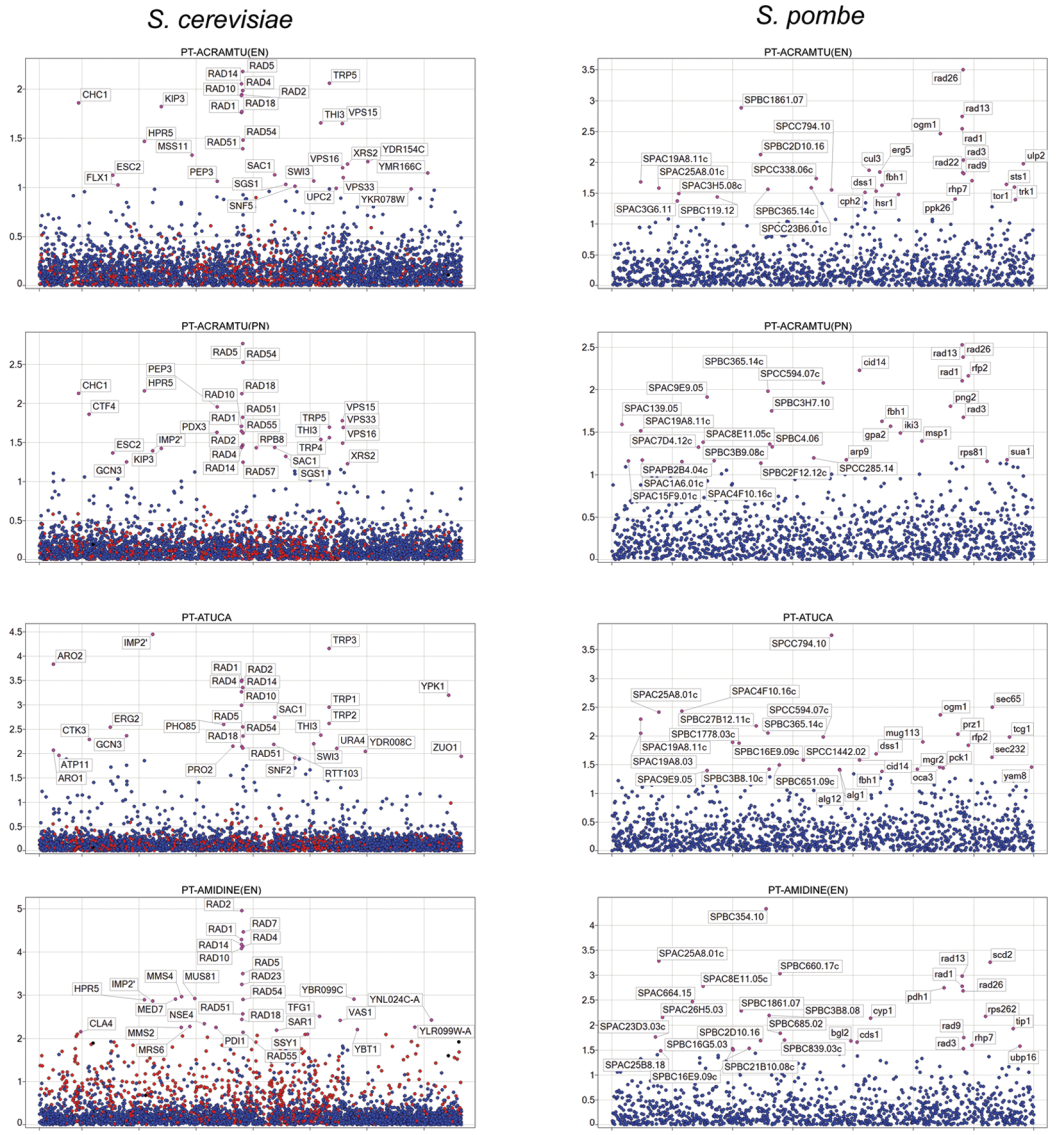

Figure 3. *S. cerevisiae* and *S. pombe* profiles for the platinum-acridine compounds that require DNA-damage response pathways. The top 30 sensitive strains are marked and labeled. Each graph represents the average of at least 3 replicate sensitivity screens in *S. cerevisiae* or 2 replicates in *S. pombe*. The *x*-axis represents gene names in alphabetical order, and the *y*-axis is the $\log_2$ ratio of barcode intensity for drug *versus* control. Red indicates essential genes, blue indicates non-essential genes, and purple indicates marked genes. Strains that often appear as hits in yeast chemogenomic assays are listed in Supplementary Table S3.

cross-linking compound. The relative ranking of strains from these five DNA-damage response (DDR) modules are shown in Figure 4a for those platinum-acridines whose profiles suggest they exert their cellular effects *via* damaging DNA. Significantly sensitive strains were tested in monoculture for compound sensitivity using fitness assays and spot dilutions with a 77% hit confirmation rate (Supplementary Tables S1, S2). To summarize the cellular responses captured by *S. cerevisiae* profiles, we performed gene set enrichment analysis (GSEA) to identify biological processes significantly enriched among genes whose deletions induce compound sensitivity, and visualized the results as a network (Supplementary Figure S1). The current state of *S. pombe* gene annotation is too sparse to permit a similar analysis.

Three of the seven platinum-intercalating hybrid derivatives of PT-ACRAMTU(EN) elicit responses from DDR genes. The bidentate non-leaving group in PT-ACRAMTU(EN) was replaced with various diamines to yield PT-ACRAMTU(PN), PT-ACRAMTU(BPY) and PT-ACRAMTU(TMEDA) (Figure 1). In previously reported *in vitro* DNA polymerase stop assays, PT-ACRAMTU(PN) and PT-ACRAMTU(BPY) were shown to produce DNA adducts.[11] Clustering of genome-wide profiles revealed that PT-ACRAMTU(PN) groups with PT-ACRAMTU(EN) and cisplatin, while PT-ACRAMTU(BPY) and PT-ACRAMTU(TMEDA) cluster separately (Figure 2). The genome-wide response to PT-ACRAMTU(PN) differed from that of PT-ACRAMTU(EN); strains deleted for genes involved in NER ranked lower in sensitivity, while strains deleted for genes involved in HRR and PRR were more sensitive. Although PT-ACRAMTU(BPY) damages DNA, we did not uncover strains deleted for DDR genes as sensitive in our screens, consistent with previously reported model studies that showed that the trans-labilizing effect of the bipyridine (BPY) ligand renders the DNA adducts formed by this compound kinetically labile.[11] Instead, PT-ACRAMTU(BPY) elicited responses for genes involved in RNA metabolic

dx.doi.org/10.1021/cb300320d | *ACS Chem. Biol.* 2012, 7, 1892–1901

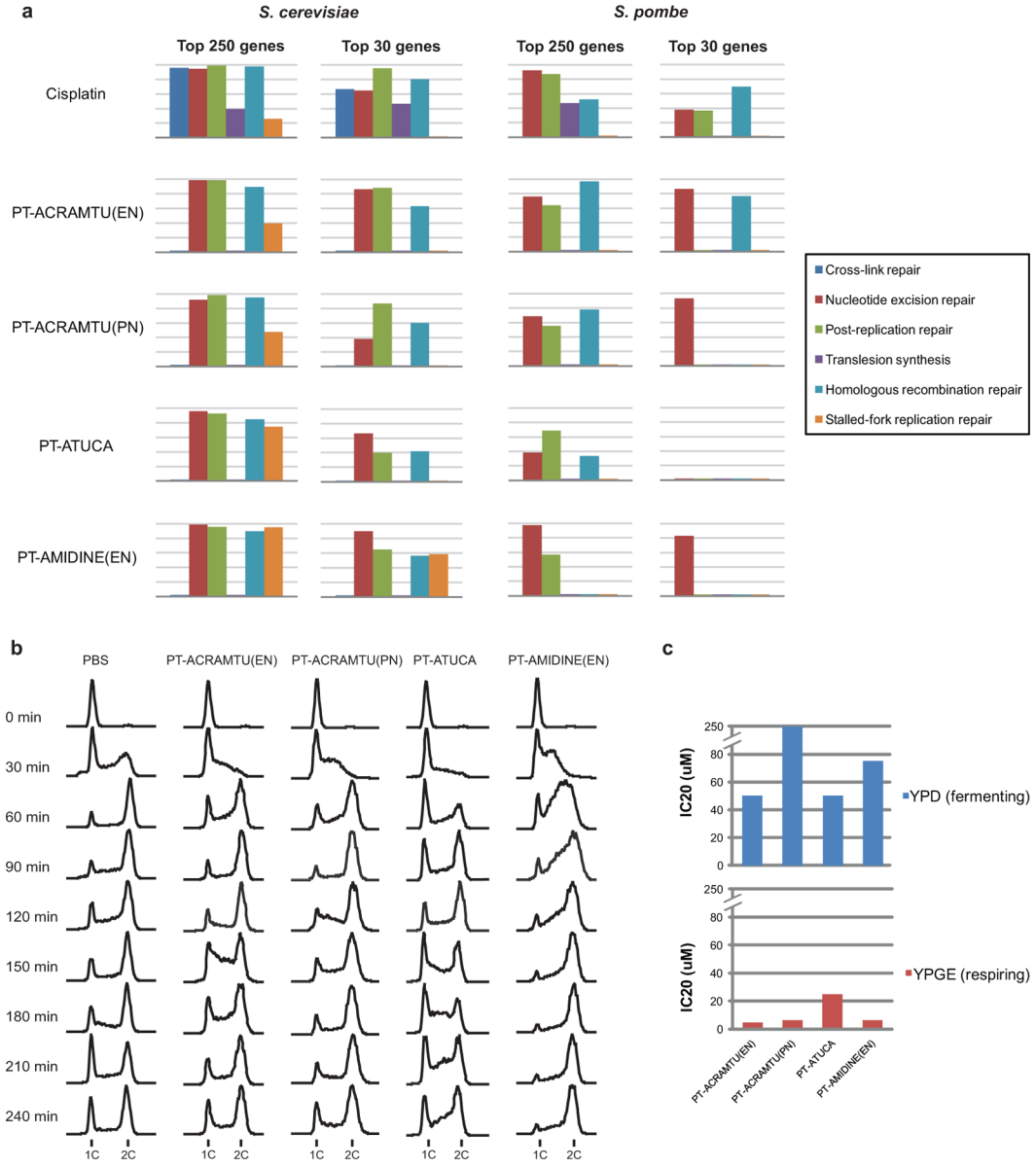

Figure 4. Four platinum-acridine compounds damage DNA, interfere with cell cycle progression, and disrupt mitochondrial function. (a) Relative importance of DNA-damage repair modules in the resistance to the DNA-damaging platinum compounds in *S. cerevisiae* and *S. pombe*. Each bar represents the median rank for genes in each of the DNA repair modules listed in the top 30 or top 250 most sensitive strains. The DNA-repair modules in *S. cerevisiae* were defined as follows: cross-linking genes (*PSO2*), NER (*RAD1*, *RAD2*, *RAD4*, *RAD10*, *RAD14*), PRR (*RAD5*, *RAD6*, *RAD18*), TLS (*REV1*, *REV3*, *REV7*), HRR (*RAD51*, *RAD52*, *RAD54*, *RAD55*, *RAD57*, *RAD59*), stalled replication fork repair (*MUS81*, *MMS4*). The DNA-repair modules in *S. pombe* were defined as follows: NER (*RHP14*, *RHP41*, *RHP42*, *RAD13*, *RAD16*, *SWI10*), PRR (*RHP6*, *RHP18*, *RAD8*), TLS (*REV1*, *REV3*, *REV7*), HRR (*RHP51*, *RHP54*, *RHP55*, *RHP57*, *RAD22*, *RTI1*), stalled replication fork repair (*MUS81*). (b) DNA content analysis profiles. Haploid BY4741 cells were synchronized at G1 prior to the addition of compound at IC_{50}. Samples were taken every 30 min after compound addition. The positions of the 1N and 2N DNA content peaks are indicated. (c) Mitochondrial function is disrupted by platinum-acridine compounds. Wildtype BY4743 cells were grown in the presence of four platinum-acridine compounds under fermenting (blue) or respiring (red) conditions. The concentration to inhibit growth by 20% (IC_{20}) is plotted.

processes. PT-ACRAMTU(TMEDA), which does not bind to DNA, did not elicit responses from any known DDR genes.

To tune the DNA sequence specificity of the monofunctional platinum moiety, the carrier group of PT-ACRAMTU(EN) was modified to produce PT-ATUCA, which features a carboxamide group attached at the 4-position of the acridine chromophore. Despite this drastic modification, the fitness profile for PT-ATUCA was similar to that of PT-ACRAMTU(EN); strains deleted for genes involved in NER, HRR, and PRR were the most sensitive (Figure 3), with NER being the most important pathway for response to this compound (Figure 4a). To generate PT-AMIDINE(EN) (the first member of this class able to slow NSCLC tumor growth in a murine xenograft[12]), the thiourea linkage was replaced with an amidine group. This seemingly minor modification resulted in greatly accelerated platinum-DNA binding[16] and reduced reactivity with cysteine sulfur, a contributor to cisplatin toxicity and tumor resistance.[17] The fitness profile for this promising lead compound featured sensitive strains deleted for genes involved in NER, HRR, and PRR. A distinct feature of this profile is that

dx.doi.org/10.1021/cb300320d | *ACS Chem. Biol.* 2012, 7, 1892–1901

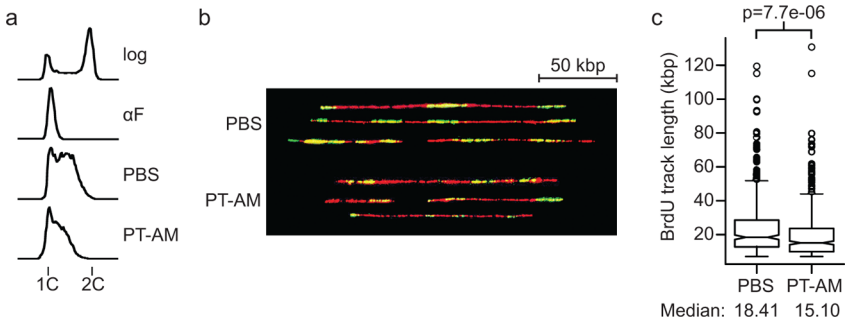

Figure 5. PT-AMIDINE(EN)-treated cells show defects in replication fork progression by DNA combing. Logarithmically growing cultures of *S. cerevisiae* cells (log) were arrested in G1 with α-factor (αF) and released in the presence of 400 μg mL^{-1} BrdU and either PBS or PT-AMIDINE(EN) (PT-AM) at IC_{50}. Samples were collected at 30 min and used in subsequent analysis. (a) DNA content analysis. Samples were fixed, and DNA contents were analyzed using flow cytometry. The positions of cells with 1C and 2C DNA contents are indicated. (b) DNA combing. Representative chromosome fibers used for replication fork progression analysis. The image is assembled from fibers on different micrographs following extraction of fibers from the nonfiber background using Adobe Photoshop. A 50 kbp scale bar is indicated in the upper right corner. (c) Distributions of BrdU track lengths in PBS- or PT-AMIDINE(EN)-treated cells, presented as a boxplot. Median BrdU track lengths are shown. The *p*-value was determined using a two-tailed Mann−Whitney U test.

two genes essential for stalled-fork repair, *MUS81* and *MMS4*, appeared in the top 15 most sensitive strains (Figure 3). Stalled-fork repair is known to be important for the cellular response to most platinum agents, yet only for PT-AMIDINE(EN) do these deletion strains rank so highly (Figure 4a). PT-ACR49NME2, where the intercalator group is modified with a DNA threading 4-carboxamide group, showed no significant gene enrichment, consistent with its low levels of DNA-binding and modest activity against cultured cells.[18]

Platinum bisintercalators were generated by replacing the chloro leaving group in PT-ACRAMTU(EN) or PT-ACR49NME2 with an ACRAMTU or ACR49NME2 moiety, respectively, yielding C-PT-BIS(ACRAMTU) and C-PT-BIS(ACR49NME2) (Figure 1). These two derivatives bind to DNA in a reversible manner by simultaneously inserting their two acridine moieties into the base stack.[10] Likely because these compounds lack a suitable leaving group and therefore do not form permanent adducts with DNA, we did not identify genes involved in DNA repair pathways in our screens. Instead, for C-PT-BIS(ACRAMTU) and C-PT-BIS(ACR49NME2) the most sensitive strains are those deleted for genes involved in vesicle-mediated transport (*AKR1*, *ARF1*, *ARL3*, *CHC1*, *MON2*, *PEP3*, *PMR1*, *RVS161*, *SUR4*, *SYS1*, *VPS15*, *VPS16*, *VPS33*, *VPS35*, *YPK1*, and *YPT31*), suggesting that transport and/or detoxification of these compounds is required for cellular resistance. The trans-isomers of these compounds, T-PT-BIS(ACRAMTU) and T-PT-BIS(ACR49NME2), did not yield any significantly sensitive hits in the screen, which may indicate limited uptake of the bulky compounds by the cells.

The recent availability of a genome-wide deletion set of *S. pombe* mutants allowed us to perform, for the first time, comparative chemogenomic characterization of a set of compounds in pooled culture. We used *S. pombe* to examine the mechanisms of cisplatin and the four compounds (PT-ACRAMTU(EN), PT-ACRAMTU(PN), PT-ATUCA, and PT-AMIDINE(EN)) that reveal DNA-damaging effects in *S. cerevisiae*. In genome-wide screens of *S. pombe*, resistance to cisplatin showed a requirement for NER, HRR, and PRR genes (Figure 4a), similar to that seen in *S. cerevisiae*. We observed that the unique requirement for TLS (*rev3*) for cisplatin resistance was also conserved in *S. pombe* (Figure 4a). The *S. pombe* deletion collection is missing 20% of genes as deletion strains, including the Δ*pso2* strain, so its role in cisplatin resistance remains to be tested. The top 250 sensitive strains in the PT-ACRAMTU(EN) and PT-ACRAMTU(PN) profiles included those deleted for genes in NER, HRR, and PRR (Figure 3, 4a). In contrast to *S. cerevisiae*, HRR (*rad22*) ranked higher than other repair modules in response to PT-ACRAMTU(EN) (Figure 4a). Furthermore, the requirement for intact PRR was less prominent than for *S. cerevisiae*, while the HRR requirement for resistance to PT-ACRAMTU(PN) treatment was conserved. Similar to *S. cerevisiae*, tolerance to PT-ATUCA required NER, HRR, and PRR, and the ranking of DDR genes was not as high as for the other compounds. PT-AMIDINE(EN) induced distinct profiles in *S. pombe* and *S. cerevisiae*; in *S. pombe*, only those strains deleted for NER and PRR genes were required for resistance. The most striking difference between the profiles from these two organisms is that *S. pombe* does not seem to require the stalled-fork repair gene *mus81* for resistance to either cisplatin or the four DNA-damaging platinum-acridine agents. Selected strains from our genome-wide *S. pombe* screens were tested for their sensitivity in monoculture with a 35% confirmation rate (Supplementary Table S1).

In light of the results from both yeasts, we asked if these agents perturb cell cycle progression. We used flow cytometry to measure DNA content in synchronized wild-type haploid *S. cerevisiae* cells that were released into each of PT-ACRAMTU-(EN), PT-ACRAMTU(PN), PT-ATUCA, and PT-AMIDINE-(EN). The compounds PT-ACRAMTU(EN), PT-ACRAMTU-(PN), and PT-ATUCA treatment slowed progression through the cell cycle (Figure 4b). Cells treated with PT-ATUCA accumulated in G1 and S phases, with only a small population of cells in G2/M at 60 min. Cells grown in PT-AMIDINE(EN) initially accumulated in S phase and only progressed through to G2/M after 90 min. Cells remained arrested in G2/M and were unable to divide and re-enter the G1 phase of the subsequent cell cycle. These cells show a distinct metaphase arrest as a result of PT-AMIDINE(EN) treatment (Supplementary Figure S2).

The observation that the *S. cerevisiae* profile of PT-AMIDINE(EN) shows an enrichment of genes involved in the replication of stalled DNA replication forks and that the cell cycle data shows slowed progression through S-phase and then accumulation at G2/M motivated us to further examine the effect of this compound on DNA replication. To examine DNA

replication fork progression directly, we performed molecular combing using synchronized *S. cerevisiae* cells. These cells, which are genetically modified to contain several copies of the Herpes Simplex Virus thymidine kinase gene, were released from G1/S synchrony into medium containing the thymidine analogue BrdU and PT-AMIDINE(EN) at an IC_{50} or into vehicle (PBS) for 30 min to allow BrdU incorporation into newly synthesized DNA. Genomic DNA was prepared, and DNA fibers were combed on silanized coverslips.[19] Replication fork progression was examined by measuring the length of BrdU tracks in the fibers. In cells treated with PT-AMIDINE-(EN) the nascent DNA tracks, as indicated by BrdU labeling, were significantly shorter compared to cells treated with the vehicle (Figure 5). This observation is consistent with PT-AMIDINE(EN) interfering with replication fork progression *in vivo*.

We further explored the cellular effects of these compounds by examining mitochondrial function and integrity following treatment. Mitochondria are often subjected to high levels of DNA damage when treated with DNA-targeting drugs. Furthermore, mitochondria are an attractive target for cancer therapy due to their role in cellular energetics and apoptosis and their derangement in different cancers. To examine whether the four DNA-damaging platinum-acridines interfere with mitochondrial function, wild-type *S. cerevisiae* cells were grown in medium that requires mitochondrial respiration (YPGE) or in a fermenting medium (YPD). In all cases, the inhibitory dose of each platinum-acridine on the cells was much lower in YPGE than YPD (Figure 4c) indicating that lack of functional mitochondria sensitizes cells to these agents. To examine whether these compounds affect mitochondrial morphology, compound-treated cells were stained with Mitotracker Red CMXRos. For each compound tested, mitochondrial morphology changed from a filamentous network to clumped vesicles (Supplementary Figure S3). Together, these results indicate that the four DNA-damaging platinum-acridines affect mitochondrial function.

In this study, we use a validated genome-wide screen to characterize novel anticancer therapeutics and explore their structure−activity relationships in an unbiased manner. The utility of *S. cerevisiae* gene deletion studies for DNA-damaging agents has been exemplified by several published studies that provide a comprehensive view of DNA repair mechanisms.[13,20,21] The results from our screens add to these reference data sets by providing a global view of the cellular response to novel agents and new insight into the activities previously attributed to these platinum-acridines including their ability to bind to DNA and their lack of a classical cross-linking mechanism for producing DNA-damage.[6,11,12,15] By classifying the DNA repair modules that were required for resistance to four of the platinum compounds, we revealed new details about their potential mechanisms at the nuclear level. The response from genes involved in NER strongly suggests that adducts generated by PT-ACRAMTU(EN) primarily lead to helical distortions in the DNA, while modification of the nonleaving group to produce PT-ACRAMTU(PN)[11] yielded a compound that appears to damage DNA *via* DNA double-strand breaks, a more severe form of DNA damage produced by either cisplatin or PT-ACRAMTU(EN). A distinctive pattern of resistance was seen in the profile of PT-AMIDINE(EN). Specifically, we found a requirement for genes involved in stalled-fork replication repair, a process that can be inhibited by DNA-damaging compounds with very different modes of action, such as alkylation, topoisomerase poisoning, and ribonucleotide reductase inhibition. In addition, PT-AMIDINE(EN), the most DNA-reactive compound in this series, causes cells to initially accumulate in S phase, a delay consistent with PT-AMIDINE-(EN) preventing or disrupting DNA synthesis, as demonstrated in NCI-H460 lung cancer cells.[22] While the three other DNA-damaging hybrid compounds featured here also slow progression of cells through S phase, the cells are able to complete the cell cycle. Our molecular combing observations suggest that the S phase delay observed with PT-AMIDINE-(EN) treatment is due, at least in part, to replication fork stalling at DNA adducts formed by this compound. In this scenario, the resumption of DNA synthesis without repair would lead to the observed cell cycle arrest at G2/M due to metaphase arrest and eventually lead to cell death. The hypothesis that severe and irreparable lesions caused by PT-AMIDINE(EN) are bypassed by DNA repair machinery frames future mechanistic studies. In addition, the mitochondrial disruption caused by each of these compounds present them as interesting candidate chemotherapeutics.[23] For example, a minor modification to the PT-ACRAMTU(EN) structure produced a compound with a cytotoxicity profile far superior to that of current platinum drugs.[12] Such pharmacophores should be of considerable interest for future clinical development.

In addition to revealing differential requirements for diverse DNA repair genes, our screens also highlight that for several platinum-acridines the mechanism by which they interfere with cellular fitness does not (primarily) involve DDR pathways. For example, the moderately cytotoxic PT-ACRAMTU(BPY) has shown some degree of coordinative binding with DNA *in vitro*, yet its fitness profile did not suggest that DNA damage results. Similar results were observed for the bis(ACRAMTU) compounds, which enter cells and inhibit cancer cell proliferation at micromolar-to-submicromolar concentrations.[24] However, the genome-wide profiles of C-PT-BIS(ACRAMTU) and C-PT-BIS(ACR49NME2) suggest that these highly charged compounds are actively detoxified by the cell and that this response is the primary means of cellular resistance. We also confirmed that bisintercalators likely do not form permanent DNA adducts on the basis of our observation that DNA repair deficient strains are not sensitive to these analogues.

The genomes of *S. pombe* and *S. cerevisiae* share many features; however, their evolutionary divergence allows for complementary functional genomic studies, particularly for examining conserved biological processes such as DNA-damage response pathways and the cell cycle, which are well-characterized in both yeast species.[25] Our genome-wide interrogation of *S. pombe* showed an array of shared and distinct cellular responses to DNA-reactive agents. The hypersensitivity of translesion repair mutants to cisplatin treatment in both yeasts emphasizes the importance of this pathway to repair DNA cross-links, while its absence in the platinum-acridine profiles further highlights the different mechanism by which they function. The PT-AMIDINE(EN) profiles in *S. cerevisiae* and *S. pombe* were similar; however, the absence of HRR deletion strains as hits in the *S. pombe* screen alludes to the presence of alternative mechanisms for resistance against PT-AMIDINE(EN)-induced double-strand breaks. Additional studies using the fission yeast deletion collection will initiate a productive cycle of gene annotation, in the same manner the accumulated genome-wide data have greatly

increased our understanding of gene function in budding yeast (for a review, see ref 26). The current study demonstrates the power of chemogenomic screening in delineating structure–activity relationships in a new class of DNA-targeted anticancer agents. The requirement for DNA-repair modules for survival of evolutionary divergent yeast cells treated with the platinating-intercalation pharmacophore unequivocally demonstrates that DNA is the principal target of these agents and gives confidence that these results can be applied in human studies. Unlike NSCLC, several cancers may be relatively insensitive to platinum-acridines. To overcome resistance in these tissues, structural designs are currently pursued which feature platinum-acridines as cytotoxic "warheads" conjugated to molecules that modulate DNA repair and/or elicit pro-apoptotic responses. Comparative chemogenomics will be an invaluable tool for studying these novel multifunctional entities.

METHODS

Reagents. Cisplatin was purchased from Sigma-Aldrich. All other compounds screened were generated according to published procedures: ACRAMTU, PT-ACRAMTU(EN),[6] ACRAMGU,[27] PT-ACRAMTU(PN/TMEDA/BPY),[11] PT-AMIDINE(EN),[12] PT-ACR49NME2,[18] PT-ATUCA,[28] C/T-PTBISACR, C/T-PTBI-SACR49NME2.[24]

Yeast Strains and Media. The *S. cerevisiae* deletion collection[29] and the *S. pombe* deletion collection[30] were used for this study. *S. cerevisiae* BY4741 and BY4743 strains were used for small-scale analyses. *S. cerevisiae* cells were grown in YPD (Yeast extract/Peptone/Dextrose), and *S. pombe* cells were grown in YES (Yeast Extract with Supplements) at 30 °C.

Deletion Pool Growth and Chip Experiments. Chemical genomic screens of the homozygous and heterozygous *S. cerevisiae* deletions pools were performed as described.[31] The same protocol was used for the *S. pombe* deletion pool. The concentrations of the compounds screened were determined using dose–response analysis on a wild-type strain. The platinum-acridine compounds were applied at a concentration that inhibits wild-type growth by 15% (200 μM for most compounds; Supplementary Figure S4). Genomic DNA preparation, PCR, and chip hybridization were performed for both yeast as described[31] with the following change: *S. pombe* samples were hybridized to the GMAP microarray.[32]

Data Analysis. (All microarray data have been deposited with Array Express, accession no. E-MTAB-1267.) Using the GeneChip Operating Software (Affymetrix), intensity values for the probes on the chip were extracted. For each strain, fitness defect ratios were calculated as the $\log_2$ of the ratio between the mean signal intensities from the control and the compound chips. The larger ratio means greater sensitivity of the strain to the compound. Complete screening data for all compounds can be found here: http://chemogenomics.med.utoronto.ca/supplemental/platinum.

Comparing Genome-Wide Profiles. The algorithm we use for comparing genome-wide profiles[14] is based on ranking of strain sensitivities and comparing a large number of full-genome profiles. Because the scale of fitness defect values of a profile can vary between profiles, a rank-based correlation of these values is advantageous. We address this challenge by scoring each profile as a series of sections, dividing each profile's gene scores into sections or "buckets", with bucket sizes modified according to significance. The smallest size bucket (0.05% of all genes) contains the most significant genes (here, genes with higher fitness defect scores), and the bucket sizes increase exponentially such that the larger size buckets contain the least significant genes, meaning those with the lowest fitness defect scores. The bucket number and sizes were the same for all profiles.

Once the genes of each profile are divided into buckets, we use a scoring matrix for scoring similarity between profiles. The scoring matrix is formulated in decreasing scores while taking into account the bucket location of each gene. When comparing profiles, the scoring matrix yields the score of $S_{i,j}$ to a gene located in bucket i and bucket j in each of the profiles compared. The scoring matrix follows these constraints:

$$\forall\ i, j | i < j \Rightarrow S_{i,i} > S_{j,j}$$

$$\forall\ i, j, k | i < j < k \Rightarrow S_{i,j} > S_{i,k}$$

Runs on a variety of data sets show that the algorithm surpasses batch effects that are common in large-scale array-based experiments.

Two-dimensional hierarchical clustering was conducted using the R statistical software package with Euclidean distance metric and the complete linkage agglomerative method.

DNA Content Analysis. Wildtype *S. cerevisiae* BY4741 cells at an OD_{600} 0.1 were arrested in G1 using 2 μg mL^{-1} α-factor for 2.5 h at 23 °C. Cells were released from the arrest and grown for an additional 2 h in the presence of compound at an IC_{50} at 23 °C. Samples were collected at half-hour time points, fixed in 70% (v/v) ethanol, and analyzed by flow cytometry as described.[33]

Molecular Combing. *S. cerevisiae* E1670 (*MAT***a** *ade2-1 trp1-1 can1-100 his3-11,15 leu2-3,112* RAD5+ GAL *psi+ ura3*::URA3/GPD-TK(7x)) cultures at an OD_{600} = 0.25 were arrested in G1 by addition of 2.5 μM α-factor for 75 min at 23 °C, followed by an additional 1 μM α-factor for 75 min. Then 400 μg mL^{-1} BrdU was added to each culture 15 min prior to compound addition. Cultures were divided and released from G1 by addition of 100 μg mL^{-1} Pronase (Sigma) and either PBS or PT-AMIDINE(EN) (350nM). Samples were collected after 30 min and incubated for 10 min in 0.1% (w/v) sodium azide on ice. Parallel samples were fixed in ethanol and analyzed by flow cytometry, as described above. Cultures were pelleted, resuspended in SCE buffer (1 M sorbitol, 100 mM sodium citrate pH = 8.5, 10 mM EDTA pH = 8.0, 0.126% (v/v) β-mercaptoethanol, 10 U mL^{-1} zymolase), and cast into 1% low melt agarose plugs to a final concentration of 3×10^8 cells mL^{-1}. Processing of DNA plugs and subsequent DNA combing and detection with anti-BrdU and anti-DNA antibodies was performed as described.[34] DNA fibers were imaged using an Axiovert inverted microscope (Carl Zeiss) with a 63x objective. Individual coverslips were blinded prior to image acquisition. Images were processed to maximize signal intensity, and fluorescent tracks were measured in Adobe Photoshop. Approximately 175 tracks were measured per sample, and track lengths were converted from pixels to kbp using a conversion factor based on combing λ DNA.[19] Experiments were repeated twice, and data from independent experiments were pooled. The distribution of track lengths was plotted as a boxplot, and the two-tailed Mann–Whitney U test was used to compare the distributions of track lengths.

ASSOCIATED CONTENT

Supporting Information

Supplementary data sets, figures, tables, and methods. This material is available free of charge *via* the Internet at http://pubs.acs.org.

AUTHOR INFORMATION

Corresponding Author

*E-mail: bierbau@wfu.edu; corey.nislow@utoronto.ca.

Notes

The authors declare no competing financial interest.

ACKNOWLEDGMENTS

We thank T. Sing for suggestions on cell cycle analysis and M. Gebbia for experimental assistance. This work was supported in part by a grant from the U.S. National Institutes of Health, CA101880 (to U.B.), from the NHGRI to C.N. and G.G., from the Canadian Cancer Society (no. 020380) to G.G. and C.N., and from the Canadian Cancer Society (no. 020254) to G.W.B. A.Y.L. was supported by a Charles H. Best fellowship.

REFERENCES

(1) Siddik, Z. H. (2003) Cisplatin: mode of cytotoxic action and molecular basis of resistance. *Oncogene 22*, 7265−7279.

(2) Kartalou, M., and Essigmann, J. M. (2001) Mechanisms of resistance to cisplatin. *Mutat. Res. 478*, 23−43.

(3) Wong, E., and Giandomenico, C. M. (1999) Current status of platinum-based antitumor drugs. *Chem. Rev. 99*, 2451−2466.

(4) Cleare, M. J., and Hoeschele, J. D. (1973) Studies on the antitumor activity of group VIII transition metal complexes. Part I. Platinum (II) complexes. *Bioinorg. Chem. 2*, 187−210.

(5) Manzotti, C., Pratesi, G., Menta, E., Di Domenico, R., Cavalletti, E., Fiebig, H. H., Kelland, L. R., Farrell, N., Polizzi, D., Supino, R., Pezzoni, G., and Zunino, F. (2000) BBR 3464: a novel triplatinum complex, exhibiting a preclinical profile of antitumor efficacy different from cisplatin. *Clin. Cancer Res. 6*, 2626−2634.

(6) Martins, E. T., Baruah, H., Kramarczyk, J., Saluta, G., Day, C. S., Kucera, G. L., and Bierbach, U. (2001) Design, synthesis, and biological activity of a novel non-cisplatin-type platinum-acridine pharmacophore. *J. Med. Chem. 44*, 4492−4496.

(7) Hess, S. M., Anderson, J. G., and Bierbach, U. (2005) A non-crosslinking platinum-acridine hybrid agent shows enhanced cytotoxicity compared to clinical BCNU and cisplatin in glioblastoma cells. *Bioorg. Med. Chem. Lett. 15*, 443−446.

(8) Hess, S. M., Mounce, A. M., Sequeira, R. C., Augustus, T. M., Ackley, M. C., and Bierbach, U. (2005) Platinum-acridinylthiourea conjugates show cell line-specific cytotoxic enhancement in H460 lung carcinoma cells compared to cisplatin. *Cancer Chemother. Pharmacol. 56*, 337−343.

(9) Baruah, H., Wright, M. W., and Bierbach, U. (2005) Solution structural study of a DNA duplex containing the guanine-N7 adduct formed by a cytotoxic platinum-acridine hybrid agent. *Biochemistry 44*, 6059−6070.

(10) Augustus, T. M., Anderson, J., Hess, S. M., and Bierbach, U. (2003) Bis(acridinylthiourea)platinum(II) complexes: synthesis, DNA affinity, and biological activity in glioblastoma cells. *Bioorg. Med. Chem. Lett. 13*, 855−858.

(11) Guddneppanavar, R., Choudhury, J. R., Kheradi, A. R., Steen, B. D., Saluta, G., Kucera, G. L., Day, C. S., and Bierbach, U. (2007) Effect of the diamine nonleaving group in platinum-acridinylthiourea conjugates on DNA damage and cytotoxicity. *J. Med. Chem. 50*, 2259−2263.

(12) Ma, Z., Choudhury, J. R., Wright, M. W., Day, C. S., Saluta, G., Kucera, G. L., and Bierbach, U. (2008) A non-cross-linking platinum-acridine agent with potent activity in non-small-cell lung cancer. *J. Med. Chem. 51*, 7574−7580.

(13) Lee, W., St, Onge, R. P., Proctor, M., Flaherty, P., Jordan, M. I., Arkin, A. P., Davis, R. W., Nislow, C., and Giaever, G. (2005) Genome-wide requirements for resistance to functionally distinct DNA-damaging agents. *PLoS Gene.t 1*, e24.

(14) Shabtai, D., Giaever, G., and Nislow, C. (2012) An algorithm for chemical genomic profiling that minimizes batch effects: Bucket Evaluations. *BMC Bioinformatics,*.

(15) Budiman, M. E., Alexander, R. W., and Bierbach, U. (2004) Unique base-step recognition by a platinum-acridinylthiourea conjugate leads to a DNA damage profile complementary to that of the anticancer drug cisplatin. *Biochemistry 43*, 8560−8567.

(16) Choudhury, J. R., Rao, L., and Bierbach, U. (2011) Rates of intercalator-driven platination of DNA determined by a restriction enzyme cleavage inhibition assay. *J. Biol. Inorg. Chem. 16*, 373−380.

(17) Ma, Z., Rao, L., and Bierbach, U. (2009) Replacement of a thiourea-S with an amidine-NH donor group in a platinum-acridine antitumor compound reduces the metal's reactivity with cysteine sulfur. *J. Med. Chem. 52*, 3424−3427.

(18) Guddneppanavar, R., Saluta, G., Kucera, G. L., and Bierbach, U. (2006) Synthesis, biological activity, and DNA-damage profile of platinum-threading intercalator conjugates designed to target adenine. *J. Med. Chem. 49*, 3204−3214.

(19) Bensimon, A., Simon, A., Chiffaudel, A., Croquette, V., Heslot, F., and Bensimon, D. (1994) Alignment and sensitive detection of DNA by a moving interface. *Science 265*, 2096−2098.

(20) St Onge, R. P., Mani, R., Oh, J., Proctor, M., Fung, E., Davis, R. W., Nislow, C., Roth, F. P., and Giaever, G. (2007) Systematic pathway analysis using high-resolution fitness profiling of combinatorial gene deletions. *Nat. Genet. 39*, 199−206.

(21) Bandyopadhyay, S., Mehta, M., Kuo, D., Sung, M. K., Chuang, R., Jaehnig, E. J., Bodenmiller, B., Licon, K., Copeland, W., Shales, M., Fiedler, D., Dutkowski, J., Guenole, A., van Attikum, H., Shokat, K. M., Kolodner, R. D., Huh, W. K., Aebersold, R., Keogh, M. C., Krogan, N. J., and Ideker, T. (2010) Rewiring of genetic networks in response to DNA damage. *Science 330*, 1385−1389.

(22) Smyre, C. L., Saluta, G., Kute, T. E., Kucera, G. L., and Bierbach, U. (2011) Inhibition of DNA synthesis by a platinum−acridine hybrid agent leads to potent cell kill in nonsmall cell lung cancer. *ACS Med. Chem. Lett. 2*, 870−874.

(23) Galluzzi, L., Larochette, N., Zamzami, N., and Kroemer, G. (2006) Mitochondria as therapeutic targets for cancer chemotherapy. *Oncogene 25*, 4812−4830.

(24) Choudhury, J. R., Guddneppanavar, R., Saluta, G., Kucera, G. L., and Bierbach, U. (2008) Tuning the DNA conformational perturbations induced by cytotoxic platinum-acridine bisintercalators: effect of metal cis/trans isomerism and DNA threading groups. *J. Med. Chem. 51*, 3069−3072.

(25) Forsburg, S. L. (2005) The yeasts Saccharomyces cerevisiae and Schizosaccharomyces pombe: models for cell biology research. *Gravity Space Biol. Bull. 18*, 3−9.

(26) Hillenmeyer, M. E., Fung, E., Wildenhain, J., Pierce, S. E., Hoon, S., Lee, W., Proctor, M., St, Onge, R. P., Tyers, M., Koller, D., Altman, R. B., Davis, R. W., Nislow, C., and Giaever, G. (2008) The chemical genomic portrait of yeast: uncovering a phenotype for all genes. *Science 320*, 362−365.

(27) Ma, Z., Day, C. S., and Bierbach, U. (2007) Unexpected reactivity of the 9-aminoacridine chromophore in guanidylation reactions. *J. Org. Chem. 72*, 5387−5390.

(28) Ma, Z., Saluta, G., Kucera, G. L., and Bierbach, U. (2008) Effect of linkage geometry on biological activity in thiourea- and guanidine-substituted acridines and platinum-acridines. *Bioorg. Med. Chem. Lett. 18*, 3799−3801.

(29) Giaever, G., Chu, A. M., Ni, L., Connelly, C., Riles, L., Veronneau, S., Dow, S., Lucau-Danila, A., Anderson, K., Andre, B., Arkin, A. P., Astromoff, A., El-Bakkoury, M., Bangham, R., Benito, R., Brachat, S., Campanaro, S., Curtiss, M., Davis, K., Deutschbauer, A., Entian, K. D., Flaherty, P., Foury, F., Garfinkel, D. J., Gerstein, M., Gotte, D., Guldener, U., Hegemann, J. H., Hempel, S., Herman, Z., Jaramillo, D. F., Kelly, D. E., Kelly, S. L., Kotter, P., LaBonte, D., Lamb, D. C., Lan, N., Liang, H., Liao, H., Liu, L., Luo, C., Lussier, M., Mao, R., Menard, P., Ooi, S. L., Revuelta, J. L., Roberts, C. J., Rose, M., Ross-Macdonald, P., Scherens, B., Schimmack, G., Shafer, B., Shoemaker, D. D., Sookhai-Mahadeo, S., Storms, R. K., Strathern, J. N., Valle, G., Voet, M., Volckaert, G., Wang, C. Y., Ward, T. R., Wilhelmy, J., Winzeler, E. A., Yang, Y., Yen, G., Youngman, E., Yu, K., Bussey, H., Boeke, J. D., Snyder, M., Philippsen, P., Davis, R. W., and Johnston, M. (2002) Functional profiling of the Saccharomyces cerevisiae genome. *Nature 418*, 387−391.

(30) Kim, D. U., Hayles, J., Kim, D., Wood, V., Park, H. O., Won, M., Yoo, H. S., Duhig, T., Nam, M., Palmer, G., Han, S., Jeffery, L., Baek, S. T., Lee, H., Shim, Y. S., Lee, M., Kim, L., Heo, K. S., Noh, E. J., Lee, A. R., Jang, Y. J., Chung, K. S., Choi, S. J., Park, J. Y., Park, Y., Kim, H. M., Park, S. K., Park, H. J., Kang, E. J., Kim, H. B., Kang, H. S., Park, H. M., Kim, K., Song, K., Song, K. B., Nurse, P., and Hoe, K. L. (2010) Analysis of a genome-wide set of gene deletions in the fission yeast Schizosaccharomyces pombe. *Nat. Biotechnol. 28*, 617−623.

(31) Pierce, S. E., Davis, R. W., Nislow, C., and Giaever, G. (2007) Genome-wide analysis of barcoded Saccharomyces cerevisiae gene-deletion mutants in pooled cultures. *Nat. Protoc. 2*, 2958−2974.

(32) Ketela, T., Heisler, L. E., Brown, K. R., Ammar, R., Kasimer, D., Surendra, A., Ericson, E., Blakely, K., Karamboulas, D., Smith, A. M.,

Durbic, T., Arnoldo, A., Cheung-Ong, K., Koh, J. L., Gopal, S., Cowley, G. S., Yang, X., Grenier, J. K., Giaever, G., Root, D. E., Moffat, J., and Nislow, C. (2011) A comprehensive platform for highly multiplexed mammalian functional genetic screens. *BMC Genomics 12*, 213.

(33) Bellay, J., Atluri, G., Sing, T. L., Toufighi, K., Costanzo, M., Ribeiro, P. S., Pandey, G., Baller, J., VanderSluis, B., Michaut, M., Han, S., Kim, P., Brown, G. W., Andrews, B. J., Boone, C., Kumar, V., and Myers, C. L. (2011) Putting genetic interactions in context through a global modular decomposition. *Genome Res. 21*, 1375−1387.

(34) Yang, J., O'Donnell, L., Durocher, D., and Brown, G. W. (2012) RMI1 promotes DNA replication fork progression and recovery from replication fork stress. *Mol. Cell. Biol. 32*, 3054−3064.

(35) Subramanian, A., Tamayo, P., Mootha, V. K., Mukherjee, S., Ebert, B. L., Gillette, M. A., Paulovich, A., Pomeroy, S. L., Golub, T. R., Lander, E. S., and Mesirov, J. P. (2005) Gene set enrichment analysis: a knowledge-based approach for interpreting genome-wide expression profiles. *Proc. Natl. Acad. Sci. U.S.A. 102*, 15545−15550.

(36) Merico, D., Isserlin, R., Stueker, O., Emili, A., and Bader, G. D. (2010) Enrichment map: a network-based method for gene-set enrichment visualization and interpretation. *PLoS One 5*, e13984.

(37) Smoot, M. E., Ono, K., Ruscheinski, J., Wang, P. L., and Ideker, T. (2011) Cytoscape 2.8: new features for data integration and network visualization. *Bioinformatics 27*, 431−432.

(38) van Dongen, S. (2000) *A cluster algorithm for graphs. Technical Report INS-R0010*, pp 1386−3681, National Research Institute for Mathematics and Computer Science in the Netherlands, Amsterdam.